

Charging of superconducting layers and resonance-related hysteresis in the current-voltage characteristics of coupled Josephson junctions

Yu. M. Shukrinov¹ and M. A. Gaafar^{1,2}¹*BLTP, JINR, Dubna, Moscow Region, RU-141980, Russia*²*Department of Physics, Faculty of Science, Menoufiya University, Egypt*

(Received 25 July 2011; published 15 September 2011)

A manifestation of a resonance-type hysteresis related to the parametric resonance in the system of coupled Josephson junctions is demonstrated. In contrast with the McCumber and Steward hysteresis, we find that the width of this hysteresis is inversely proportional to the McCumber parameter and it also depends on the coupling between junctions and the boundary conditions. Investigation of the time dependence of the electric charge in superconducting layers allows us to explain the origin of this hysteresis by different charge dynamics for increasing and decreasing bias current processes. The effect of the wavelength of the longitudinal plasma wave created at the resonance on the charging of superconducting layers is demonstrated. We find a strong effect of the dissipation in the system on the amplitude of the charge oscillations at the resonance.

DOI: [10.1103/PhysRevB.84.094514](https://doi.org/10.1103/PhysRevB.84.094514)

PACS number(s): 74.81.Fa, 74.20.De, 74.50.+r, 74.78.Fk

I. INTRODUCTION

The hysteresis features of the single Josephson junction (JJ) have been studied by McCumber and Steward a long time ago.^{1,2} Particularly, it was shown that the width of the hysteresis was determined by the capacitance of the JJ being proportional to the McCumber parameter β_c related to the dissipation parameter β by $\beta_c = 1/\beta^2$. The origin of the hysteresis becomes clear if we take into account the analogy in the behavior of JJ and massive particle in the “washboard” potential (see, for example, Ref. 3). In comparison with the single junction, the system of the coupled Josephson junctions has a multiple branch structure in its current-voltage characteristics (CVC), and the definition of the return current characterizing the hysteresis is more general now: the system can return to the zeroth voltage state from any branch. The outermost branch of CVC has a breakpoint (BP) and a breakpoint region (BPR) before a transition to another branch reflected by the parametric resonance in the system.⁴

It was shown by Koyama and Tachiki⁵ that the system of equations for capacitively coupled Josephson junctions has a solution corresponding to the longitudinal plasma wave (LPW) propagating along the c axis. So the Josephson oscillations can excite LPW by their periodic actions.⁶ The frequency of Josephson oscillations ω_J is determined by the junction voltage, and is at $\omega_J = 2\omega_{LPW}$, where ω_{LPW} is LPW frequency, where the parametric resonance is realized. It means that the BP current characterizes the resonance point at which LPW with a definite wave number is created in the stack of JJs.

The hysteresis features of the intrinsic JJ in high temperature superconductors are of great interest also due to the observed powerful coherent radiation from that system.⁷ In Ref. 8, the authors summarized the experimental results and stressed that the strong emission was observed near the unstable point of the return current in the uniform voltage branch. The radiation was related to the same region in the CVC where BP and BPR were observed. This made the phase dynamics investigation of the intrinsic JJ corresponding to these parts of CVC an urgent problem today.

Since the thickness of the superconducting layer (S layer) in the intrinsic JJ is comparable to the Debye screening length,

the S layers are in the nonstationary nonequilibrium state due to the injection of quasiparticle and Cooper pairs.^{5,9} The charge neutrality in S layers is locally broken and this charging effect modifies the Josephson relation between the voltage and the phase difference. The questions of the value of the electric charge in the S layer and its maximum realized at the parametric resonance have not been investigated yet.

In this paper, we study the phase dynamics in coupled Josephson junctions. A resonance-type hysteresis related to the parametric resonance in this system is demonstrated. We show that the width of this hysteresis is inversely proportional to the McCumber parameter and depends on the coupling parameter of the system and the boundary conditions. The origin of this hysteresis is related to the different charge dynamics for increasing and decreasing bias current processes. We discuss the question concerning the maximal electric charge in S layers realized at the resonance and show that it depends on the relation between the wavelength of LPW and the period of lattice. We demonstrate a strong effect of the dissipation in the system on the coefficient of the exponential growth of the maximal electric charge in S layers.

The paper is organized in the following way. In Sec. II, we introduce the coupled sine-Gordon equation, which is used for numerical simulations and discuss the boundary conditions and a numerical procedure. In Sec. III, we present the results of simulation of CVC demonstrating the hysteretic behavior and its features near the parametric resonance region. To clarify the origin of the hysteresis, we describe the time dependence of the charge oscillations in the S layers in Sec. IV. In Sec. V, we discuss the question concerning the amplitude of the electric charge oscillations in the S layer at the parametric resonance and show that its maximal value depends on the wavelength of created LPW. In Sec. VI, the charge-time dependence in the growing region at different dissipation magnitudes is presented. Finally, we discuss the obtained results and come to the conclusions.

II. MODEL AND METHOD OF CALCULATION

Let us consider the system of $N + 1$ superconducting layers in anisotropic high- T_c superconductors. The thicknesses of

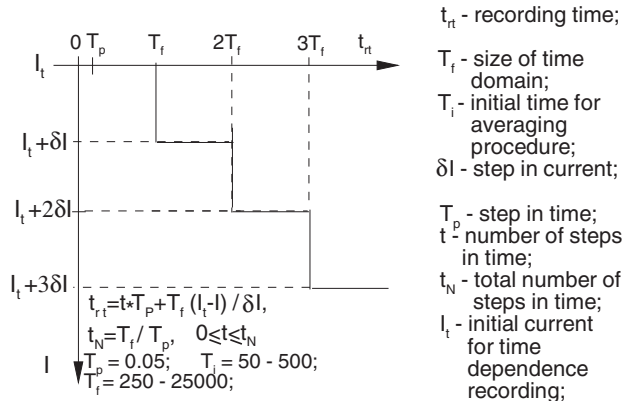


FIG. 1. Scheme of the numerical procedure for the phase dynamics investigation in coupled Josephson junctions.

and then down. A change in these parameters greatly changes the branch structure in CVC. Their influence on CVC in the framework of the CCJJ and CCJJ + DC models was discussed in Refs. 11–13. To calculate the voltages $V_l(I)$ at each point of CVC (for each value of I), we simulate the dynamics of the phases $\varphi_l(t)$ by solving the system of equations (2) using the fourth-order Runge-Kutta method with a step in time T_p . The scheme of the numerical procedure and parameters of simulation are presented in Fig. 1. After simulation of the phase dynamics we calculate the dc voltages on each junction as

$$\partial\varphi_l/\partial t = \sum_{l'} A_{ll'} V_{l'}, \quad (5)$$

where V_l is normalized to $V_0 = \hbar\omega_p/(2e)$. The average of the voltage \bar{V}_l is given by

$$\bar{V}_l = \frac{1}{T_f - T_i} \int_{T_i}^{T_f} V_l dt, \quad (6)$$

where T_i and T_f determine the interval for the temporal averaging. After completing the voltage averaging for bias current value I , the current value is increased or decreased by a small amount of δI (bias current step) to calculate the voltages in all junctions at the next point of CVC. We use the distribution of phases and their derivatives achieved at the previous point of CVC as the initial distribution for the current point.

Numerical stability was checked by doubling and dividing in half the temporal discretization steps T_p and checking the influence on the CVC. Finally, we can obtain the total dc voltage V of the stack by

$$V = \sum_{l=1}^N \bar{V}_l. \quad (7)$$

At some bias current value some junction (or junctions) switches to the nonzero voltage state and gives some branch of CVC. We plot the total CVC at different parameters of the problem. The details concerning the numerical procedure are given in Refs. 11–13. To investigate the BPR in detail, we have calculated CVC for different boundary conditions for stacks with a different number N of IJJs.

III. HYSTERETIC BEHAVIOR NEAR BREAKPOINT

The results of simulation of CVC and its features near the parametric resonance region are presented in Fig. 2(a). The inset to this figure shows the total branch structure of CVC for the stack with 9 JJs at $\alpha = 1$, $\beta = 0.2$, and nonperiodic boundary conditions with $\gamma = 0.5$. We stress the following features of CVC: (i) a jump at $I/I_c = 1.0$ from the zero-voltage branch to the outermost branch with all junctions in the rotating state, (ii) practically linear dependence of the voltage on the bias current at $I > I_c$, and (iii) multiple branching in the hysteresis region. The circle and arrow with letter B show the BP location on the outermost branch.

Figure 2(a) shows part of the total CVC of the stack and demonstrates a hysteresis in the outermost branch. It is obtained by decreasing the bias current to some point in BPR (curve 1), then we increase the current to pass the resonance region again (curve 2). The arrows show the direction of the bias current change. The hysteresis is characterized by its width $I_{B^*} - I_B$, where I_B is the value of the breakpoint current in the decreasing current process and I_{B^*} is a characteristic current value in the increasing current process.

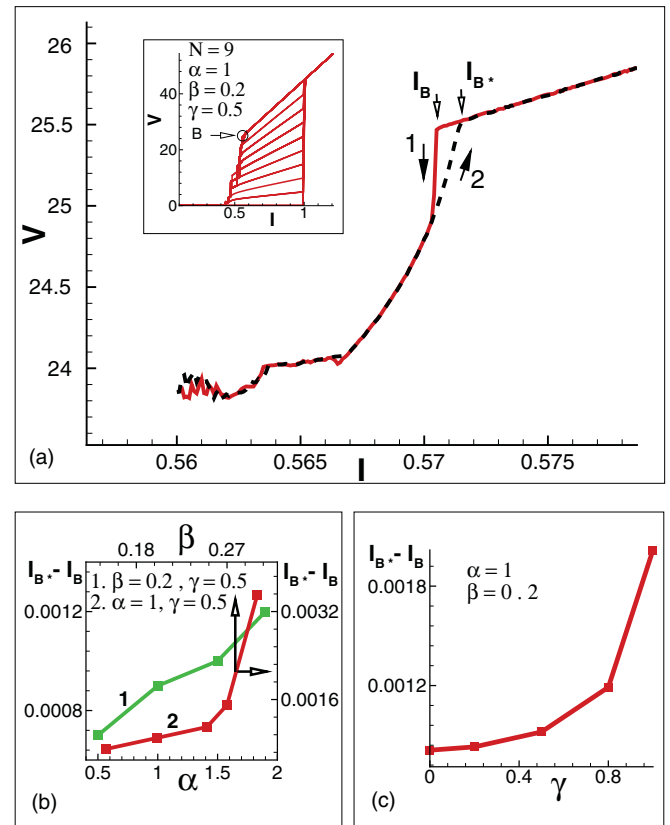


FIG. 2. (Color online) (a) Demonstration of the hysteresis behavior in the parametric resonance region in the outermost branch of the CVC for the stack with 9 JJs at $\alpha = 1$, $\beta = 0.2$, and $\gamma = 0.5$. The arrows show the direction of the bias current sweeping. The inset shows the total branch structure in the CVC of this stack and BP location; (b) shows a change of the hysteresis width $I_{B^*} - I_B$ with the dissipation parameter β and coupling parameter α , and (c) shows the same with variation of the nonperiodic parameter γ .

The dependence of the hysteresis width on the dissipation parameter β is shown in Fig. 2(b) (the corresponding axes shown by arrows). The width increases with the parameter β , i.e., it decreases with the McCumber parameter. As we mentioned above, this result is in contrast with the McCumber and Stewart hysteresis for a single JJ. They obtained that the return current I_r (which characterizes the value of hysteresis) decreases with increasing of McCumber parameter.¹¹ So we have observed a resonance-type hysteresis related to the parametric resonance in coupled JJs. In Ref. 14, we showed that the origin of the very small details in CVC was related to the details of the charge dynamics in the superconducting layers. Below we demonstrate that this hysteresis can be explained by different charge dynamics for decreasing and increasing bias current processes in obtaining CVC in the resonance region. Figures 2(b) and 2(c) also show an increase in the hysteresis width $I_{B*} - I_B$ with the coupling parameter α and parameter of nonperiodicity γ .

IV. TIME DEPENDENCE OF CHARGE OSCILLATIONS IN THE S-LAYERS

To make clear the origin of this hysteresis, we study the time dependence of the charge oscillations in the S-layers. Using the Maxwell equation $\text{div}(\epsilon\epsilon_0 E) = Q$, where ϵ_0 is the permittivity (electric constant), we express the charge density

$$Q_l = Q_0\alpha(V_{l+1} - V_l) \quad (8)$$

in the S layer l by the voltages V_l and V_{l+1} in the neighboring insulating layers, where $Q_0 = \epsilon\epsilon_0 V_0 / r_D^2$. The solution of the system of dynamical equations for phase differences gives us the voltages as functions of time $V_l(t)$ in all junctions in the stack and it allows us to investigate the time dependence of the charge in each S layer. As we mentioned above, the charge dynamics in the S layers determines the features of the current voltage characteristics of the coupled Josephson junctions.¹⁴ Here, we investigate the charge-time dependence for two processes: decreasing [see Figs. 3(a), 4–6] and increasing [see Fig. 3(b)] the bias current through the stack. The recorded time is calculated as

$$t_{rt} = t + T_f(I_0 - I)/\delta I \quad (9)$$

for the decreasing bias current process. For the increasing current process [see Fig. 3(b)], we record the time dependence at bias current value I during the time interval $(t_{rt}, t_{rt} - T_f)$. The simulations were done at $T_f = 1000$, $T_p = 0.05$, and $\delta I = 0.0001$.

In Fig. 3, the time dependence of the charge in the S layer of the stack with nine coupled JJs at $\alpha = 1$, $\beta = 0.2$, and periodic BC is combined with CVC of the outermost branch. We see the characteristic fine structure in the breakpoint region of CVC and the corresponding features in the charge-time dependence. The arrows show the direction of the bias current sweeping. Here and after, we present the charge oscillations in the first S layer of the stack; the features of the charge oscillations we are interested in are practically the

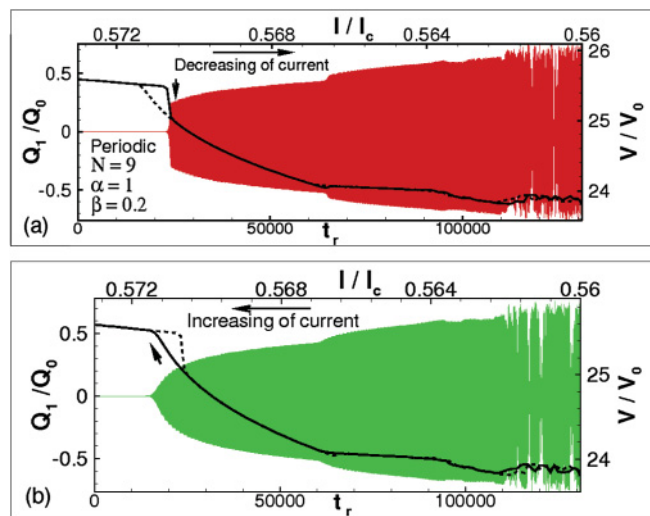


FIG. 3. (Color online) Difference in the charge-time dependence and CVC in (a) the decreasing current process and (b) the increasing current process. The thick curves (solid and dashed) show CVC.

same in all other layers. Figure 3(a) shows the charge-time dependence when the current approaches the resonance point in the decreasing current process, while Fig. 3(b) presents it when the bias current is increased. We can see that the charge on the S layer in Fig. 3(b) disappears at a different value of current in comparison with the current value in the decreasing process [see Fig. 3(a)]. So the origin of the observed hysteresis is related to the parametric resonance in this system and different charge dynamics in the superconducting layers for decreasing and increasing bias current sweeping in obtaining CVC.

V. LPW WITH DIFFERENT WAVELENGTH

Let us now discuss the question concerning the amplitude of the electric charge oscillations in the S layer at the parametric resonance, which corresponds to BP on the outermost branch of CVC. Does its maximal value depend on the wavelength of created LPW?

As was shown in Ref. 5, the system of equations for CCJJ has a solution corresponding to LPW propagating along the c axis. Frequency of LPW at the bias current $I = 0$ and $\beta = 0$ is given by

$$\omega_{\text{LPW}}(k) = \omega_p \sqrt{1 + 2\alpha(1 - \cos kd)} \quad (10)$$

where k is the wave vector of LPW and $d = d_s + d_I$ is the period of the stack of Josephson junctions. At point B [see Fig. 2(a)] the Josephson oscillations excite LPW by their period actions. The frequency of Josephson oscillations is determined by the voltage value in the junction, so at $\omega_J = 2\omega_{\text{LPW}}$ the parametric resonance is realized and LPW is created.

The Josephson oscillations excite LPW with $k = \pi/d$ (π -mode, wavelength $\lambda = 2d$) at the parametric resonance in the stack with an even number of JJs at $\alpha = 1$, $\beta = 0.2$ and periodic BC.⁶ However, in the stacks with an odd number of

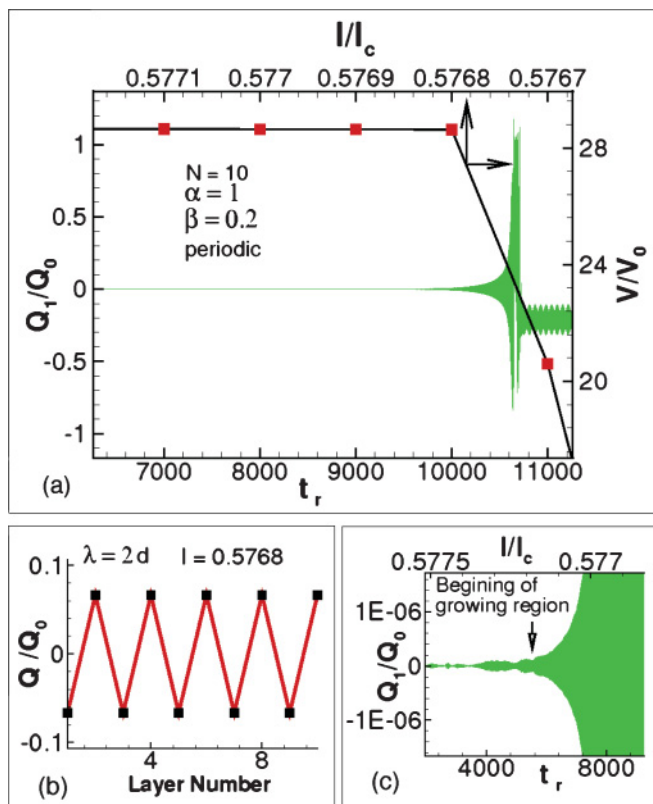


FIG. 4. (Color online) (a) Demonstration of the absence of fine structure in charge-time dependence and CVC for the stack with ten junctions at $\alpha = 1$, $\beta = 0.2$, and periodic BC. The filled squares mark the bias current steps in CVC. (b) Charge distribution among the layers. (c) The beginning of the growing region of the charge in the S layer.

JJs the wave number depends on the number of junctions N and it is equal to $k = \pi(N - 1)/dN$. In the stacks with an even number of JJs the resonance is “pure,” i.e., no additional fine structure appears in CVC.¹⁵ So it is interesting to compare the maximal value of the electric charge realized in S layers in this case (N even) with the case $\lambda \neq nd$ (N odd), where n is an integer number.

In Fig. 4(a), we present the time dependence of the electric charge in the S layer for the stack with 10 JJs combined with the outermost branch of CVC (the corresponding axes are shown by arrows). We found that the bias current interval where the growing region [the beginning of that region is demonstrated in the Fig. 4(c)] of the electric charge in S layers is observed, is shorter now in comparison with the $N = 9$ case, where LPW with $k = 8\pi/9d$ is created at the same values of α and β . Comparing this figure with Fig. 3 for $N = 9$, we can see that the amplitude of the charge is larger for the stack with an even number of JJs. Figure 4(b) illustrates the charge distribution among the layers and confirms the π mode of LPW. As we mentioned above, the wavelength of LPW depends on the values of the dissipation and coupling parameters.⁴ So we can compare the stacks with 9 and 10 JJs when LPW with different wave numbers are created and test the idea concerning the maximal amplitude of charge oscillations in the S layer.

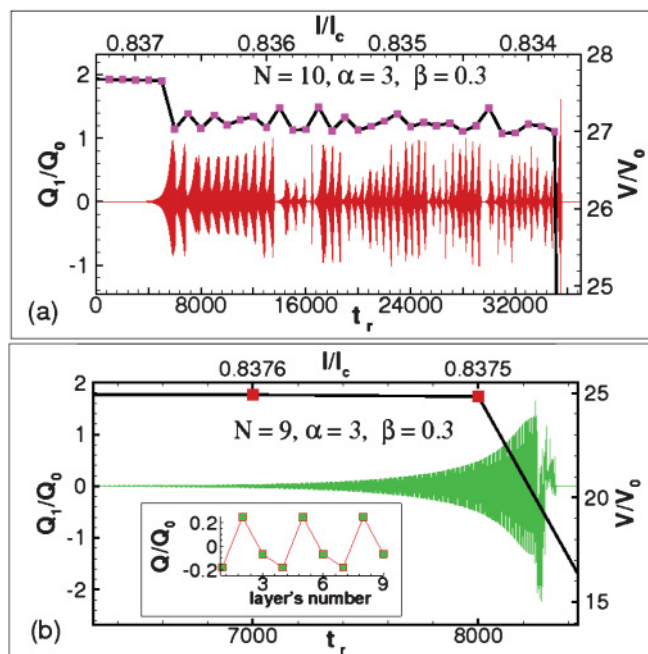


FIG. 5. (Color online) Charge-time dependence and CVC at $\alpha = 3$, $\beta = 0.3$, and periodic BC: (a) for a stack with 10 JJs and (b) for a stack with 9 JJs. The inset shows the charge distribution among the layers corresponding to the $2\pi/3d$ mode in the stack with 9 JJs.

In Fig. 5, the time dependence of the charge in the first S layer at $\alpha = 3$, $\beta = 0.3$, and the periodic BC combined with CVC of the outermost branch are presented. Figure 5(a) shows these dependencies for the stack with 10 junctions. The CVC demonstrates BPR with irregular variation of the voltage reflecting a complex charge dynamics in the S-layers. We stress that at chosen values of parameters $\alpha = 3$ and $\beta = 0.3$ LPW with $k = 3\pi/5d$ is created.⁴ The corresponding wavelength does not satisfy the condition $\lambda = nd$. In the case $N = 9$ [see Fig. 5(b)], the inset illustrates the charge distribution among the layers corresponding to the $(2\pi/3d)$ mode ($\lambda = 3d$). It leads to the absence of the fine structure in CVC in the parametric resonance region.

We can see that the charge value on the S layers in the $k = 2\pi/3d$ case is larger than in the case of $k = 3\pi/5d$, which is the same result as we got before. In addition, we tested the cases for $\lambda = 4d$ and $\lambda = 5d$ (not presented here) and they supported our idea as well. So we may conclude that at the fixed α and β the charge value in the S layers is larger for the stacks with the pure parametric resonance, where LPW with $\lambda = nd$ is created.

VI. CHARGE-TIME DEPENDENCE IN THE GROWING REGION

To demonstrate the character of the charge amplitude increasing in the growing region, we enlarged in Fig. 6 the charge-time dependence for the stack with 10 JJs at $\alpha = 1$ and $\beta = 0.2$.

In the inset (a), we present the time dependence of the normalized amplitude of the charge in the first layer Q_1^A/Q_0 in the logarithmic scale. The values of the amplitude were

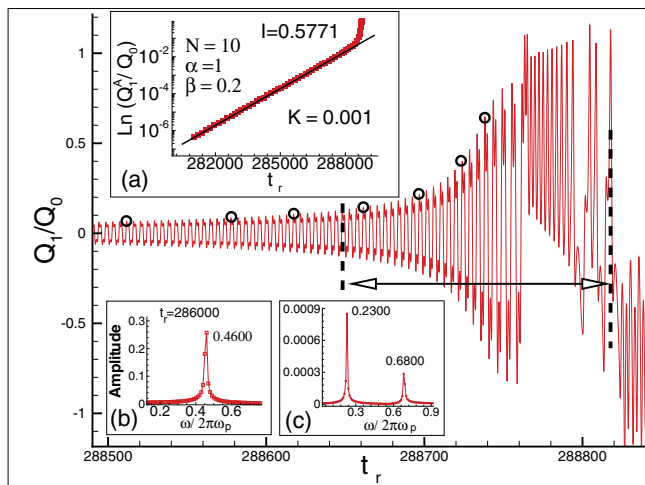


FIG. 6. (Color online) Demonstration of the transition part (shown by double arrow) in charge-time dependence for the stack with 10 JJs. The inset (a) shows the amplitude of charge oscillations in the logarithmic scale. The insets (b) and (c) demonstrate the results of the FFT analysis of the voltage $V(t)$ and charge $Q_1(t)/Q_0$ time dependence in the exponential growth part.

taken at arbitrary times in the total growing region (examples are shown by circles in Fig. 6). There are two different parts in the charge-time dependence in Fig. 6: exponential part and transition part (marked by double arrow) before a jump to another branch. In the transition part the amplitude demonstrates a sharp increase in a short time interval in comparison with the exponential part. The insets (b) and (c) show the results of the fast Fourier transform (FFT) analysis of the voltage $V(t)$ and charge $Q_1(t)/Q_0$ time dependence in the exponential growth part. They prove the parametric resonance condition $\omega_J = 2\omega_{\text{LPW}}$. In the transition part, this condition is broken. Writing the expression for the electric charge as

$$Q_1/Q_0 = \exp(Kt) \quad (11)$$

we find $K = 0.001$.

Figure 7 illustrates the influence of the dissipation magnitude ($\beta = 0.2, 0.1$, and 0.05) on the time dependence of the charge oscillation amplitude in the logarithmic scale for the stack with ten junctions at $\alpha = 1$. From this figure, we see the following features that are observed with decrease in β (increase in the McCumber parameter): (i) the growing region is getting shorter, (ii) the width of the transition part decreases; and (iii) the coefficient of the exponential growth K increases. We come to the important conclusion that the parametric resonance features depend strongly on dissipation in the system. The width of the growing region is inversely proportional to the coefficient K . The value of K is determined by the wave number of LPW created at the resonance. As we mentioned above, in the stacks with an even number of junctions at $\alpha = 1$, $\beta = 0.2$, and periodic BC, the wave number of LPW is the same ($k = \pi/d$). In agreement with this, for all investigated stacks with an even number of JJs (in our simulations we checked the stacks

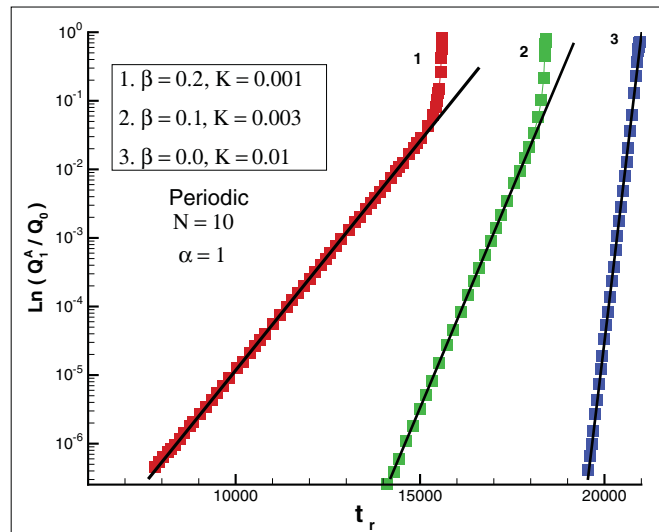


FIG. 7. (Color online) Influence of the dissipation magnitude on the time dependence of the charge oscillation amplitude in the logarithmic scale for the stack with ten junctions at $\alpha = 1$.

with $N = 4, 6, 8, 10, 12$, and 14) we obtained the same value of $K = 0.001$. However, as we showed before, for stacks with a fixed number of junctions, parameter K depends strongly on β .

The animation of the charge dynamics at different time moments in the growing region demonstrates the standing π mode of the created LPW (the charge on the nearest neighbor layers has the same value and an opposite sign) in the exponential part and its modification in the transition region.¹⁶ The corresponding avi files are given in Supplemental Material.¹⁶

As a summary, the manifestation of a resonance-type hysteresis related to the parametric resonance in the system of coupled Josephson junctions is demonstrated. The width of this hysteresis is inversely proportional to the McCumber parameter and depends on the coupling between junctions and the boundary conditions. The origin of this hysteresis is related to the different charge dynamics for the increasing and decreasing bias current processes. We consider that these features are common for the systems demonstrating the parametric resonance. These features can be used to develop the methods for determination of coupling and dissipation parameters of the system. We show that the maximal value of the electric charge amplitude realized in superconducting layers at the resonance depends on the wavelength of the created LPW. A strong effect of the dissipation in the system on the width of the parametric resonance is demonstrated.

ACKNOWLEDGMENTS

We thank I. Rahmonov, M. Hamdipour, S. Nedelko, H. El Samman, S. Maize, M. Elhofy, and Kh. Hegab for helpful discussions and support of this work.

- ¹D. E. McCumber, *J. Appl. Phys.* **39**, 3113 (1968).
- ²W. C. Stewart, *Appl. Phys. Lett.* **12**, 277 (1968).
- ³A. Barone and J. Paterno, *Physics and Applications of the Josephson Effect* (Wiley, New York, 1982).
- ⁴Yu. M. Shukrinov and F. Mahfouzi, *Phys. Rev. Lett.* **98**, 157001 (2007).
- ⁵T. Koyama and M. Tachiki, *Phys. Rev. B* **54**, 16183 (1996).
- ⁶Yu. M. Shukrinov and F. Mahfouzi, *Supercond. Sci. Technol.* **20**, S38 (2007).
- ⁷L. Ozyuzer *et al.*, *Science* **318**, 1291 (2007).
- ⁸T. Koyama, H. Matsumoto, M. Machida, and K. Kadowaki, *Phys. Rev. B* **79**, 104522 (2009).
- ⁹D. A. Ryndyk, *Phys. Rev. Lett.* **80**, 3376 (1998).
- ¹⁰R. Kleiner, F. Steinmeyer, G. Kunkel, and P. Muller, *Phys. Rev. Lett.* **68**, 2394 (1992).
- ¹¹Yu. M. Shukrinov and F. Mahfouzi, *Physica C* **434**, 6 (2006).
- ¹²H. Matsumoto, S. Sakamoto, F. Wajima, T. Koyama, and M. Machida, *Phys. Rev. B* **60**, 3666 (1999).
- ¹³Yu. M. Shukrinov, F. Mahfouzi, and P. Seidel, *Physica C* **449**, 62 (2006).
- ¹⁴Yu. M. Shukrinov, M. Hamdipour, and M. R. Kolahchi, *Phys. Rev. B* **80**, 014512 (2009).
- ¹⁵Yu. M. Shukrinov, F. Mahfouzi, and M. Suzuki, *Phys. Rev. B* **78**, 134521 (2008).
- ¹⁶See Supplemental Material at <http://link.aps.org/supplemental/10.1103/PhysRevB.84.094514> for access to avi files, showing the animation of the charge dynamics at different time moments in the growing region.